**Light Metals 2015**
*Edited by: Margaret Hyland*
***TMS (The Minerals, Metals & Materials Society), 2015***

# Light Metals 2015

## STRIP CASTING OF LIGHT METALS

## Modeling and Properties

*SESSION CHAIRS*
**Dietmar Letzig**
Helmholtz-Zentrum Geesthacht
Geesthacht, Germany

**Murat Dündar**
Assan Aluminium
Istanbul, Turkey

**Light Metals 2015**
*Edited by: Margaret Hyland*
***TMS (The Minerals, Metals & Materials Society), 2015***

# MODELLING OF THE TWIN ROLL CASTING PROCESS INCLUDING FRICTION

Dag Mortensen[1], Hallvard G. Fjær[1], Dag Lindholm[1], Kai F. Karhausen[2], Jakob S. Kvalevåg[3]

[1]Institute for Energy Technology, P.O. Box 40, N-2027 Kjeller, Norway
[2]Hydro Aluminium Rolled Products, Georg-von-Boeselager-Strasse 21, D-53014 Bonn, Germany
[3]Hydro Aluminium Rolled Products, Karmøy Rolling Mill, Hydrovegen 160, N-4265 Håvig, Norway

Keywords: Twin Roll Casting, Modelling, Friction, Solidification, Roll force, Forward slip

## Abstract

Twin roll casting is a combined solidification and deformation process and the material flow is thereby more complex than in many other casting processes. A modelling approach is presented including heat and fluid flow coupled with stresses and deformations. A Coulomb friction law is applied and by iterations on the mechanical conservation equations the parts of the cast surface that are either in slip or sticking mode against the roll shell are determined and tangential forces are calculated. Results like the total roll force and the forward slip on the strip are available from the model. Generally the model approach is applicable to both aluminium and magnesium casting with the appropriate material characteristics. In this study a 2D finite element simulation on the twin roll casting of a 1050 alloy is performed and the calculated roll force and forward slip are compared with results from industrial TRC processing trials.

## Introduction

The knowledge and detailed quantification of material flows in the twin roll casting process is of interest for further development of the process. Increasing alloy content is restricted by macrosegregation caused by mechanical deformation of the mushy zone [1]. Also the thermo-mechanical behavior of the strip and the roll shell is important for optimization and productivity of aluminium and magnesium strip production [2,3]. The process uses a minimum of energy by going directly from liquid melt to thin plates and together with low investment costs this causes a considerable interest in the industry for further exploiting the twin roll casting process [4]. The modelling tool described here, called Alsim, has been developed specifically for continuous casting processes applied in the industry [5-10].

## Modelling

Due to the simultaneous solidification and deformation the material flow in twin roll casting is more complex than in most other solidification processes. The computational node movement in Alsim for this process is adapted to the roll shell speed, while the real material flow is calculated with the mechanical model. A 2D finite element approach is applied, as the heat flow in the width direction is assumed to be insignificant and a plane strain-approximation is assumed to be valid for a large part of the strip.

### Heat and fluid flow

The model for the heat and fluid flows is based on a continuum mixture model for the solid-liquid material. A Darcy force is used in the mixture momentum equations that accounts for the interfacial friction due to the different velocities of the solid and the liquid. The mixture incompressible formulation for time-dependent flows including turbulence is given below including a solidification term which accounts for the friction between liquid and solid:

$$\frac{\partial u_i}{\partial x_i} = 0 \tag{1}$$

$$\frac{D_\omega u_i}{\partial t} + (u_j - \omega_j)\frac{\partial u_i}{\partial x_j} = -\frac{1}{\rho_0}\frac{\partial p}{\partial x_i} + \frac{\partial}{\partial x_j}(\nu + \nu_t)\frac{\partial u_i}{\partial x_j} + f_i + S_i - \frac{2}{3}\frac{\partial \kappa}{\partial x_i}$$

where $u_i$, $\omega_i$, p, $\nu$, $\nu_t$, $\rho_0$ and $\kappa$ are the mixture velocity, the computational node velocity, the pressure, the kinematic viscosity, the turbulent kinematic viscosity, the density and the turbulent energy, respectively. $D_\omega/\partial t$ denotes the time derivative of a variable moving with the velocity of the computational grid. More details about the Boussinesq buoyancy term $f_i$ , the Darcy type solidification term $S_i$ and the LRN-k-ε turbulence model may be found in [6]. The following mixture formulation is applied for energy conservation, including the internal heat generation:

$$\frac{\mathrm{D}_\omega}{\partial t}(\rho h) - \omega_j \frac{\partial}{\partial x_j}\left(\rho^l g^l h^l + \rho^s g^s h^s\right) + \frac{\partial}{\partial x_j}\left(\rho^l g^l h^l u_j^l + \rho^s g^s h^s u_j^s\right) = \frac{\partial}{\partial x_j}\lambda\frac{\partial}{\partial x_j} + \sigma_{ij}\dot{\varepsilon}_{ij}^{vp} \tag{2}$$

where h, λ, T, σ and $\varepsilon^{vp(dot)}$ are the enthalpy, the heat conductivity, the temperature, the stress tensor and the viscoplastic strain rate tensor.

### Stresses and deformations

The basic equation in the stress modelling is Cauchy's equation for the momentum balance where the inertia terms are neglected:

$$\nabla \cdot \boldsymbol{\sigma} = \rho \mathbf{g} \tag{3}$$

The material is treated as an elastic-viscoplastic material for which plasticity and creep are treated in a uniform manner. The thermal contractions were neglected in this study. The stresses are only solved for the cast metal and the rolls are treated as rigid.. The total strain rate $\dot{\boldsymbol{\varepsilon}}$ is derivable from the time derivative of the displacement field **u,** and it is subdivided into a viscoplastic and elastic component.

$$\dot{\boldsymbol{\varepsilon}} = \frac{1}{2}\left(\nabla\dot{\mathbf{u}} + \left[\nabla\dot{\mathbf{u}}\right]^T\right) = \dot{\boldsymbol{\varepsilon}}^{vp} + \dot{\boldsymbol{\varepsilon}}^{e} \tag{4}$$

As the solid material is not attached to the mesh, the algorithm used for solving the solid momentum balance in DC casting [5] must be modified. Instead of using the total displacement field as unknowns, the increments for the displacement in the current time

step is applied here. The elastic strain can then be written as the sum of the elastic strains in the last time step computed by an up-winding scheme and the increment in the current time step:

$$\boldsymbol{\varepsilon}^{e,n+1} = -\left(u_i - \omega_i\right)\frac{\partial \boldsymbol{\varepsilon}^{e,n}}{\partial x_i} + \dot{\varepsilon}^{e}\Delta t \qquad (5)$$

The constitutive equation for elasticity (Hook's law) defines how the stress depends on the elastic strain $\boldsymbol{\varepsilon}^e$ and the temperature dependent Young's modulus and Poisson's ratio entering the matrix **D.**

$$\boldsymbol{\sigma} = \mathbf{D}(T)\cdot\boldsymbol{\varepsilon}^{e} \qquad (6)$$

A set of equations assuming steady state creep above a temperature $T_0$ and work hardening below this temperature, was applied here:

$$\bar{\sigma} = F\left(T\right)\cdot\left(\phi_0 + \phi\right)^{n(T)}\cdot\left(\dot{\bar{\varepsilon}}_p\right)^{m(T)} \qquad (7)$$

$$d\phi = \begin{cases} d\bar{\varepsilon}_p & \text{when} \quad T \le T_0 \\ 0 & \text{when} \quad T > T_0 \end{cases} \qquad (8)$$

Treatment of the mesh

Various parts of the computational domain relate to different kinematic descriptions, see Figure 1. For melt in the nozzle and in the meniscus that bridges the nozzle outlet to the roll contact point, fluid flow and enthalpies are solved in a fixed Eulerian mesh. A single column of elements makes the expander zone where elements continuously grow from an initial size. When their length exceeds a critical length, the elements are divided into two and the procedure is repeated. The front elements in the expander column join the elements in the roll bite which are updated (moved) in an Arbitrary Lagrangian Eulerian (ALE) system. In order to reduce the size of the problem and to keep the computational cost low, columns of elements are removed from the domain when they passes a certain position after the center of the roll gap (roll bite). Elements that are continuously squeezed through the roll bite moves as a combination of rotation and translation. During one time step a nodal point moves the distance ΔS from the old position S1 (S=Strip) to a the new position S2 according to

$$\Delta S = a\cdot(D/2)\cdot\omega\cdot\Delta t + (1-a)\cdot\Delta O \qquad (9)$$

where D is the roll outer diameter, ω is the angular velocity of the roll, Δt is the time step size, ΔO is the distance along the symmetry plane in the casting direction and a function of the rotation from R1 to R2 (see Figure 1). This equation also includes the dimensionless parameter a, which is defined as the ratio between the distance S1-O1 to R1-O1. The average nodal velocity during the time step is then ΔS/Δt. Nodes in the roll shell are moved in an ALE coordinate system as a pure rotation.

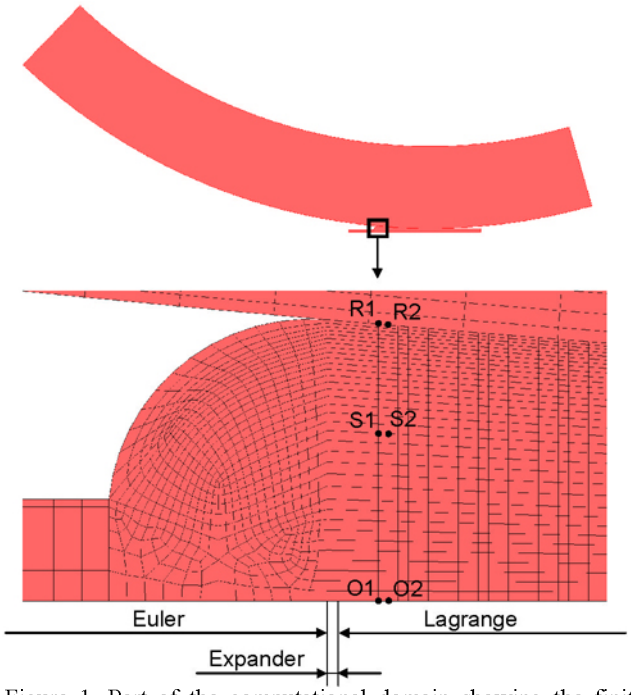


Figure 1. Part of the computational domain showing the finite element grid at the entrance to the roll gap (nozzle, meniscus, roll shell and strip)

Thermo-fluid-mechanical coupling

The solid flow from the solid momentum equations is solved first in each time step including friction against the roll shell. The fluid mass and momentum equations are then solved next with friction against the solid flow through the Darcy term in these equations. The energy equation with the enthalpy formulation including internal heat generation from friction is solved in the end of the time step.

The calculation of mechanical friction forces involves finding the parts of the cast surface that are either in slip or sticking mode against the roll shell. An iterative algorithm is applied. For each time step there is an initial guess on slip or sticking for different parts of the surface. A guess on the tangential forces for nodes in the slip regions is made from forces in the previous time step. Then plastic strains in the bulk is found and normal and sticking tangential forces are calculated. For any node on the sticking surface, the normal residual force multiplied with the friction coefficient has to be larger than the tangential force in order for the iterative process to be converged. Correspondingly, on the part of the surface with slip the normal force multiplied with the friction coefficient should correspond to the applied tangential force. If the computed velocity of the cast metal relative to the roll is found to be in opposite to the applied tangential force, either the force is increased, or sticking is assumed. If no change of nodal sticking/slip is required, and the relative change of the sum of tangential forces (absolute values) is less than a user defined criterion (here 0.001), the iteration is considered to be converged. Typically, 3-4 iterations on the boundary conditions were required for each time step. A typical result is shown in Fig. 4. The part of the surface marked with red shows the calculated sticking zone while before the sticking zone the cast surface moves slower than

the roll shell and after the sticking zone the cast surface moves faster.

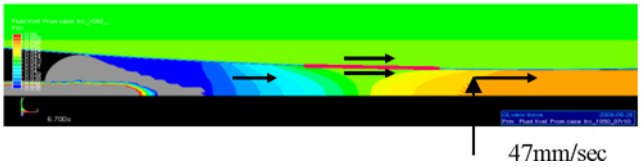


Figure 2. Cast and roll speed in a twin roll casting example showing calculated sticking zone marked red. Speed (material speed) contours are from 35mm/sec to 50mm/sec in steps 1mm/sec. Last contour line is at 47mm/sec (marked with an arrow). Speed (fluid flow speed) out of range is shown with grey color.

Material properties and thermal boundary conditions

Thermal properties for an AA1050 alloy were calculated by the microstructure model Alstruc [11]. For the mechanical properties the F(T), n(T) and m(T) functions in equation (7) were taken from merging the low strain rate data in [12] and the high strain rate data in [13]. Since no direct measurements from the roll shell were available the measured strip temperature out of the rolls were used to tune ad hoc the angle dependent heat transfer coefficients from the strip against the rolls (ranging from 6kW/m$^2$K to 240kW/m$^2$K). A copper roll shell was used with thermal conductivity as for pure copper.

## Experiments

Data from 4 casting trials with metallurgical pure aluminium on a full scale Pechiney machine were used [14]. The strip was 6mm thick, set-back of the nozzle was 45mm from the roll bite, roll shell diameter was 931mm, the produced strip width was 1486mm in average. The tension in the strip was estimated to be 10 tons (and used as the mechanical boundary condition for the end of the strip in the model). The roll speed was in average ~2600mm/min. The average measured separating force was 743tons and the average measured forward slip (extra speed on strip compared to roll speed) was 6.2%. The measured temperature on the cast strip surface approximately 1m from the roll gap was in average about 220ºC.

## Results

A "standard case" was set up using the experimental data above. The 2D computational domain was selected using only the tip of the metal distributor, a static meniscus from the tip to the roll shell and a half strip (assuming symmetry although that is not completely true considering the fluid flow part with natural convection). The static meniscus was estimated assuming the contact angle between the meniscus and the roll is 180°. The strip geometry expands with the roll shell speed but elements are cut off at a distance equal to 40mm from the roll bite. On the cut plane a mechanical boundary condition is applied corresponding to the strip tension. For the roll shell only a 60° section was applied. As it takes a long time for a full roll shell to develop a stationary temperature field only a smaller section was used but with a start temperature corresponding to the estimated stationary temperature of the roll shell as it approaches the strip. Figure 3 shows the development in the temperature field from the start of the simulation until ~stationary conditions are reached. Figure 4 shows the calculated velocities in the fluid flow part.

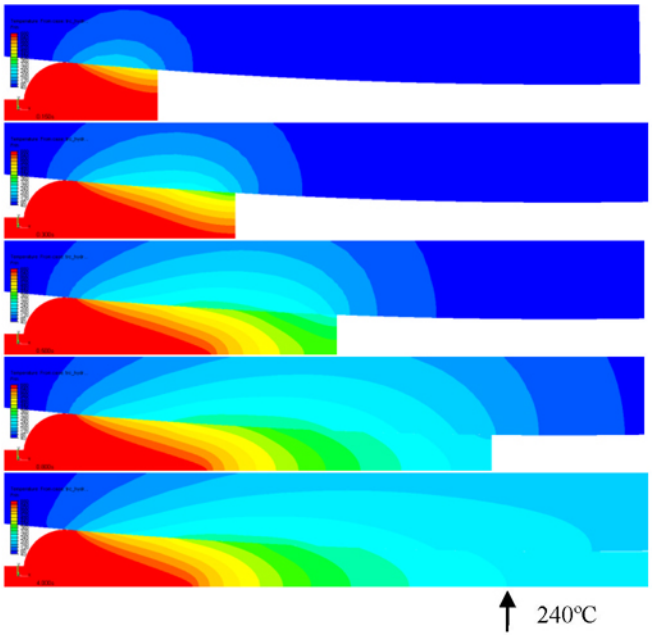


Figure 3. From top: Thermal development at 0.15, 0.3, 0.5, 0.8 and 4seconds from start of casting. At 4 seconds close to stationary conditions has been reached in the strip for the temperatures and the stresses. Temperature contours are from 40 to 680ºC with step 40ºC.

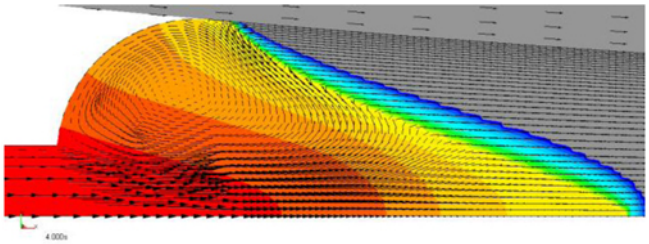

Figure 4. Fluid flow field and solid velocity field in strip and roll shell. The maximum arrow size corresponds to the max velocity out of the center of the tip (109mm/sec). Temperature contours here from 600 to 680ºC in steps 5ºC.

Results for the stresses are shown in Figure 5. The shift from tensile to compressive shear stresses defines the neutral plane in the rolling part of the strip after end of solidification in the center.

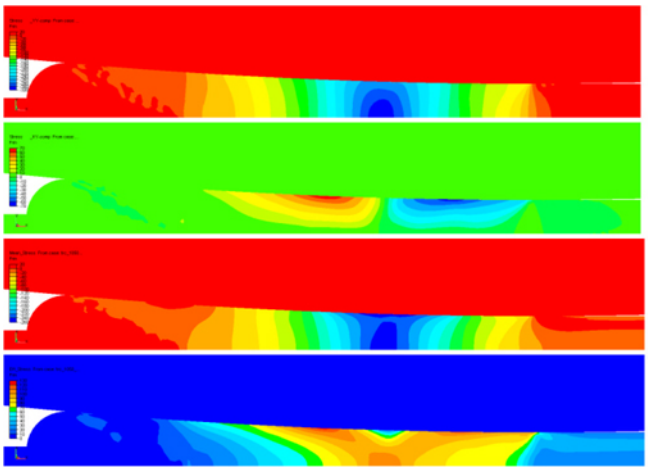

Figure 5. From top: Vertical (YY-) component of stress tensor, contours from -320 to 20MPa in steps 20MPa. Shear (XY-) component of stress tensor, contours from -70 to 70MPa in steps 10MPa. Mean (average) stress, contours from -260 to 20MPa in steps 20MPa. Effective stress, contours from 0 to 130MPa in steps 10MPa.

Figure 6 shows the computed distribution of the normal and tangential stress along the roll shell. The start and end of the sticking zone between strip and roll shell are identified as well as the neutral plane. Before the start of the sticking zone the roll shell moves faster than the solid strip material so effectively pushing the solid while after the end of the sticking zone the roll shell moves slower than the solid strip material so effectively decelerating the surface of the solid.

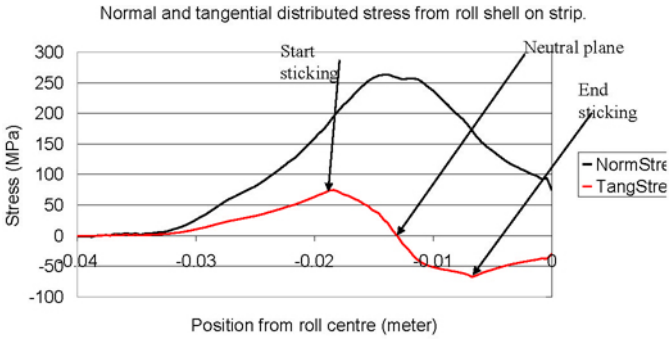


Figure 6. Normal and tangential stress in MPa along the roll shell surface as function of horizontal distance from the roll bite.

By integrating normal stress along the roll shell a good comparison was found between the calculated roll force and the measured roll forces in the cast house, the calculated roll force was 714tons compared to the average of 743tons in the four casting trials. Also the calculated forward slip (the speed difference between the strip and the roll shell) confirmed well with cast house data. The applied friction coefficient was 0.4 and the calculated forward slip ("extrusion") was 6.9% compared to the average of 6.2% in the four casting trials. The calculated torque on the roll was 76kNm.

A small sensitivity study was performed varying some of the parameters. In Case 1 the friction coefficient was reduced from 0.4 to 0.3. In Case 2 the tension in the strip was reduced from 10tons to 1ton. In Case 3 the flow stress in the constitutive equation from [12,13] was increased with 20%. Table 1 shows the computed roll forces, torques and forward slip for these cases.

| Case | Roll Force (tons) | Torque on roll (kNm) | Forward slip (%) |
|---|---|---|---|
| Std | 714 | 76 | 6.9 |
| 1 | 608 | 60 | 6.4 |
| 2 | 746 | 98 | 6.5 |
| 3 | 858 | 95 | 6.9 |

Table 1. Result of case study on roll force, torque and forwards slip.

A parameter of interest is how much the material is strained. Figure 7 shows the thermal field and the accumulated effective strain for three cases, the standard case and a +/- 20% variation on the roll speed. A 20% reduction in speed results in 24% higher maximum straining of the material while a 20% increase in speed results in 20% reduction of the maximum straining.

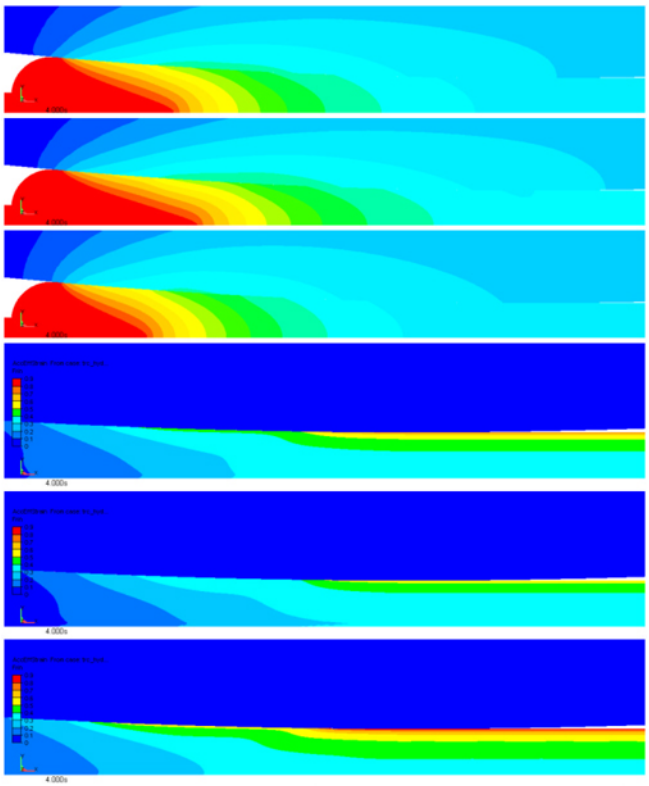

Figure 7. From top: Thermal fields at stationary conditions for the standard case, 20% increase in roll speed and 20% decrease in roll speed. Temperature contours are from 40 to 680ºC with step 40ºC. Accumulated effective strain for the standard case, 20% increase in roll speed and 20% decrease in roll speed. Contours are from 0 to 0.9 with step 0.1.

## Discussion

The removal of heat against the roll shell has only been validated in average. Lacking data on the detailed surface temperature of the strip and/or the roll shell we could estimate an average heat loss by imposing heat transfer coefficients as function of angle in such a way that we reach the measured strip temperature after casting. Naturally we then start with a comparably low heat transfer coefficient close to the meniscus region where the pressure is low and we are increasing this heat transfer coefficient as we approach the center of the gap, but this choice has been ad hoc. Anyhow, using these heat transfer coefficients we are computing the correct strip temperature, and using published data on the flow stress as function of temperature, strain and strain rate we end up with a good estimate of the roll force and the forward slip. The deviations in the standard case from the average casting trial results are 4% for the roll force and 11% for the forward slip.

In order to calculate also macrosegregation in twin roll casting and other microstructural parameters the heat transfer to the rolls has to be validated more closely. A pressure and shear stress dependency for the heat transfer coefficients could be used if there are experimental data to validate such an approach. Also the meniscus movement is of interest regarding the surface properties. Future developments of the modelling tool will concentrate on surface heat transfer, meniscus dynamics and mechanically induced macrosegregation.

## Conclusions

A thermo-fluid-mechanical finite element model including friction for the twin roll casting process has been validated against industrial casting trials. Results regarding the total roll force and the forward slip of the strip are in good comparison with plant data using the correct temperature in the strip, a friction coefficient equal 0.4 and published material data for thermo-elastoviscoplastic constitutive models for commercial pure aluminium.

## Acknowledgements

Funding of this work partly by the EUREKA project E!3725 Casting Top Models (CTM) and partly by Hydro Aluminium is gratefully acknowledged. The mathematical model Alsim used in this study is currently under development in the Alsim/Primal-project with participation from Alcoa Norway ANS, Aleris Rolled Products Germany GmbH, Norsk Hydro ASA, Institute for Energy Technology and SINTEF Materials and Chemistry, and with support from the Research Council of Norway.

## References

[1] O. Grydin, M. Stolbchenko, F. Nürnberger, M. Schaper, "Influence of the twin-roll casting parameters on the microsegregation in thin strips of the aluminium alloy EN AW-6082", Light Metals 2014, TMS, Warrendale PA, pp411-414.
[2] M. Dündar, B. Beyhan, O. Birbasar, H.M. Altuner, "Surface crack characterization of twin roll caster shells and its influence on as-cast strip surface quality", Light Metals 2013, TMS, Warrendale PA, pp491-495.
[3] A. Hadadzadeh, M.A. Wells, "Mathematical modelling of thermo-mechanical behavior of strip during twin roll casting of an AZ31 magnesium alloy", Journal of Magnesium and Alloys 1 (2013), pp101-114.
[4] E. Romano, C. Romanowski, "Reinventing twin roll casting for the 21st century", Light Metals 2009, TMS, Warrendale PA, pp895-900.
[5] H.G. Fjær, A. Mo, "ALSPEN – A mathematical model for thermal stresses in DC casting of aluminium billets", Metall. Trans. 21B (1990), pp1049-1061.
[6] D. Mortensen, "A mathematical model of the heat and fluid flows in direct-chill casting of aluminium sheet ingots and billet", Metall. Trans. 30B (1999), pp.119-133.
[7] M. M'Hamdi, A. Mo and H.G. Fjær, "TearSim: A two-phase model addressing hot tearing formation during aluminium direct chill casting", Metall. Trans. A, 2006, vol.37A, pp.3069-3083.
[8] J. Grandfield, S. Dablement, H. Fjaer, D. Mortensen, M. Lee, V. Nguyen and G. Savage, "3D thermo-mechanical modeling of wheel and belt continuous casting", Materials Science Forum, 693 (2011), pp.235-244.
[9] M. Turski, A. Paradowska, S-Y. Zhang, D. Mortensen, H. Fjaer, J. Grandfield, B. Davis and R. DeLorme, "Validation of predicted residual stresses within direct chill cast magnesium alloy slab", Metall. Trans. 43A (2012), pp.1547-1557.
[10] D. Mortensen, M. M'Hamdi, K. Ellingsen, K. Tveito, L. Pedersen, G. Grasmo, "Macrosegregation modelling of DC-casting including grain motion and surface exudation", Light Metals 2014, TMS, Warrendale PA, pp867-872.
[11] A.L. Dons et.al., Metall. Trans. A, 1999, vol.30A, pp.2135-2146.
[12] W.M. van Haaften, "Constitutive behaviour and hot tearing during aluminium DC casting", PhD-Thesis TUDelft, The Netherlands, 2002. ISBN 90-9015792-1.
[13] W.A. Wong, J.J. Jonas, Trans. of the Metall. Soc. of AIME 242 (1968) 2271-2280.
[14] B. Forbord, B. Andersson, F. Ingvaldsen, O. Austevik, J.A. Horst, I. Skauvik, "The formation of surface segregates during twin roll casting of aluminium alloys", Materials Sci. and Eng. A 415 (2006), pp.12-20.